A dominant-negative form of POM121 binds chromatin and disrupts the two separate modes of nuclear pore assembly

Lihi Shaulov, Rita Gruber, Ilana Cohen and Amnon Harel*

Department of Biology, Technion – Israel Institute of Technology, Haifa 32000, Israel

*Author for correspondence (amharel@tx.technion.ac.il)

Accepted 1 July 2011
Journal of Cell Science 124, 3822–3834

doi: 10.1242/jcs.086660

Summary

Nuclear pore complexes (NPCs) are formed during two separate stages of the metazoan cell cycle. They are assembled into the re-forming nuclear envelope (NE) at the exit from mitosis and into an intact, expanding NE during interphase. Here, we show that a soluble internal fragment of the membrane nucleoporin POM121 has a dominant-negative effect on both modes of assembly in a cell-free reconstitution system. The soluble POM121 fragment binds chromatin at sites that are distinct from ELYS–Nup107–160 'seeding' sites and prevents membrane enclosure and NPC formation. Importin-β negatively regulates chromatin binding by the POM121 fragment through a conserved NLS motif and is also shown to affect the recruitment of the endogenous membrane protein to chromatin in the full assembly system. When an intact NE is present before the addition of the dominant-negative fragment, NPCs are inserted into the NE but membrane expansion is inhibited. This results in densely packed NPCs with no intervening membrane patches, as visualized by scanning electron microscopy. We conclude that POM121 plays an important role in both modes of assembly and links nuclear membrane formation and expansion to nuclear pore biogenesis.

Key words: Cell cycle, Nuclear envelope expansion, Nuclear pore assembly, POM121

Introduction

The nuclear pore complex (NPC) is an intricate biological machine that mediates bidirectional transport of macromolecules across the nuclear envelope (NE) (Fahrenkrog et al., 2004; Gerace and Burke, 1988; Hetzer and Wente, 2009; Weis, 2003). NPCs are embedded at the junction of the two nuclear membranes and are composed of multiple copies of ~30 different proteins termed nucleoporins (Nups) (Alber et al., 2007; Cronshaw et al., 2002; Vasu and Forbes, 2001). Open mitosis in higher eukaryotes entails the synchronous assembly of NPCs and the nuclear envelope (NE) in a tightly regulated, stepwise process, which is coordinated with other mitotic exit events (Burke and Ellenberg, 2002; Guttinger et al., 2009; Wozniak and Clarke, 2003). NPCs also form at a separate stage of the metazoan cell cycle, by insertion into the intact NE during interphase (D'Angelo et al., 2006). This second mode of NPC formation enables metazoan cells to double NPC numbers during interphase (Maul et al., 1972) and more closely resembles the assembly pathway of lower eukaryotes, which undergo a closed mitosis (Fernandez-Martinez and Rout, 2009; Ryan et al., 2007).

The individual subunits that make up the massive structure of the NPC comprise three to four integral membrane Nups and 12–15 distinct subcomplexes of soluble Nups in different eukaryotes (Alber et al., 2007; Chadrin et al., 2010; Hetzer and Wente, 2009; Rasala et al., 2008; Schwartz, 2005). The mechanistic details and sequence of events in NPC assembly have been a matter of controversy and debate. Although NPC biogenesis is often described as a self assembly process, there is also evidence for the involvement of additional assembly factors, such as importin-β (Harel et al., 2003a; Ryan et al., 2007; Walther et al., 2003). The Nup107–160 complex is known to bind to chromatin through the adaptor protein ELYS and form the initial seeding sites, or 'prepores', for postmitotic NPC assembly (Franz et al., 2007; Gillespie et al., 2007; Rasala et al., 2006; Rasala et al., 2008; Rotem et al., 2009), but subsequent steps remain obscure. Moreover, extensive redundancy has been suggested to exist in the roles of specific proteins in assembly, especially in the case of integral membrane Nups (Stavru et al., 2006a).

Integral membrane Nups are thought to provide stable anchoring points for the mature NPC within the specialized, highly curved pore-membrane domain. In addition, these membrane nucleoporins have been suggested to play specific roles in NPC assembly, such as recruiting soluble Nups to the initial assembly sites and triggering fusion of the inner and outer nuclear membrane (Antonin et al., 2005; Drummond and Wilson, 2002; Fichtman et al., 2010; Macaulay and Forbes, 1996; Mitchell et al., 2010; Stavru et al., 2006b). A persistent problem has been the lack of overall phylogenetic conservation in sequence and topology of the integral membrane Nups. NDC1, which has six membrane-spanning segments, is the best conserved membrane Nup that is present in yeast and metazoa, but apparently absent from protozoa (Mansfeld et al., 2006; Stavru et al., 2006a). In yeast, NDC1 is a component of both the NPC and the spindle pole body (SPB), and fulfils the essential function of enabling the insertion of newly formed SPBs into the intact NE (Chial et al., 1998; Lau et al., 2004). gp210 is a type I

transmembrane protein with a large luminal domain located between the inner and outer nuclear membranes, a single membrane-spanning segment and a short cytoplasmic tail (Gerace et al., 1982; Wozniak et al., 1989). This protein is evolutionarily conserved in metazoa and found in some protozoa and plants, but is missing in fungi (Stavru et al., 2006b). POM121 is the least conserved of the three vertebrate membrane Nups. It has the opposite topology to gp210, with a single membrane-spanning segment close to its N-terminus and the bulk of the protein facing the NPC channel. POM121 orthologues have only been identified in vertebrates (Antonin et al., 2005; Funakoshi et al., 2007; Hallberg et al., 1993).

There is conflicting evidence regarding the vital function for each of the three vertebrate membrane Nups in NPC assembly (Antonin et al., 2005; Cohen et al., 2003; Doucet et al., 2010; Drummond and Wilson, 2002; Funakoshi et al., 2011; Mansfeld et al., 2006; Stavru et al., 2006a; Stavru et al., 2006b). Most recently, POM121 has been proposed to play a crucial, rate-limiting role in interphase NPC assembly but not in the postmitotic process (Doucet et al., 2010). This contrasts with a previous suggestion that POM121 functions as part of a postmitotic checkpoint mechanism that coordinates NPC assembly with the formation of a fully enclosed NE (Antonin et al., 2005). Multiple inner nuclear membrane proteins have been suggested to bind directly to chromatin and drive membrane recruitment by collaborative and possibly redundant interactions (Anderson et al., 2009; Ulbert et al., 2006). In addition, reticulons and other membrane-bending and deforming proteins play a crucial role in ER expansion into an enclosed NE (Anderson and Hetzer, 2008), and might also be required for the insertion of NPCs into membranes in the de novo (interphase) mode of assembly (Dawson et al., 2009).

Collectively, the experimental results from different systems and partially conflicting reports indicate that both modes of NPC assembly are intricate, multi-step processes involving many components. As pointed out by Stavru et al. redundancies and built-in back up mechanisms can easily obscure the function of a given protein in such complicated settings (Stavru et al., 2006a). This is particularly relevant for experiments relying on RNAi-mediated knockdown of specific Nups in mammalian cells, or immunodepletion in cell-free reconstitution systems.

We sought an alternative strategy to study the role of POM121 in nuclear assembly. We reasoned that introducing a soluble fragment, lacking the transmembrane segment of POM121, into an in vitro assembly system might disrupt crucial interactions of the endogenous protein and help to reveal its functions. Here we describe such dominant-negative interactions of a soluble POM121 domain, affecting both the postmitotic and interphase modes of NPC assembly.

Results

A dose-dependent inhibitory effect of a soluble POM121 fragment

Cell-free systems derived from amphibian egg extracts have long served as an experimental model to study postmitotic NPC assembly (Antonin et al., 2005; Forbes et al., 1983; Harel et al., 2003b; Lohka and Masui, 1983; Rotem et al., 2009; Walther et al., 2003) and can also be used to follow NPC insertion into intact membranes (D'Angelo et al., 2006; Harel et al., 2003a; Vollmar et al., 2009). To test for a potential dominant-negative effect in the nuclear reconstitution assay, we expressed several fragments of *Xenopus laevis* POM121, lacking the transmembrane segment, as recombinant GST fusion proteins in bacteria (supplementary material Fig. S1A). Purified, soluble fragments were introduced into the full assembly system, containing chromatin, cytosol and membrane components. This analysis focused our attention on one central fragment, encompassing amino acids 143–415, which had a strong inhibitory effect on nuclear assembly. This region shows 41% identity to rat POM121 and contains an internal sequence of ~35 more highly conserved residues (Fig. 1A) with a recently characterized bipartite nuclear localization signal (NLS) (Doucet et al., 2010). The purification and characterization of the soluble GST-POM121$^{143–415}$ fusion protein is described in supplementary material Fig. S1B,C. We refer to this soluble fragment as POM121^{DN}.

When POM121^{DN} was added to the full assembly system at $t=0$, a dose-dependent inhibitory effect on nuclear assembly was observed (Fig. 1B). Control nuclei stained strongly with mAb414, an antibody that recognizes a group of phenylalanine–glycine repeat nucleoporins (FG Nups) in mature NPCs, and accumulated a fluorescent classical NLS import cargo (Fig. 1B, top row). No NPC staining or import were observed in reactions that contained 10 μM or higher concentrations of the POM121 fragment, a result that was comparable to full inhibition by the calcium chelator BAPTA. To determine whether the aborted assembly intermediates were enclosed by continuous, fully fused membranes we performed an identical set of assembly reactions with fluorescently labeled membrane vesicles (Fig. 1C). After 1 hour of assembly, both the control nuclei and BAPTA-inhibited intermediates were encircled by a continuous membrane stain, whereas a discontinuous membrane rim was observed in the presence of POM121^{DN} (Fig. 1C, bottom row). This suggested a possible defect in membrane vesicle fusion on the surface of chromatin.

POM121^{DN} prevents membrane enclosure

We next performed a time-course experiment to follow the kinetics of membrane recruitment to the chromatin templates in the cell-free assembly system. Membrane recruitment and fusion were largely complete by 20 minutes in both the control and BAPTA reactions (Fig. 2A). A substantial delay in membrane recruitment was observed in assembly reactions containing 10 μM POM121^{DN}, with a discontinuous membrane rim staining seen at 30 minutes. This suggests that the discontinuous membrane staining observed at 1 hour (Fig. 1C) could be the result of a failure to recruit a specific subtype of membrane vesicles (see Discussion). Nuclear assembly intermediates that were incubated in the presence of the POM121^{DN} fragment were also fragile and showed an increased sensitivity to handling of the solution in the samples removed between 30–60 minutes of incubation. To circumvent this problem we used the anchored chromatin assembly method, in which chromatin templates are attached to a solid support before being exposed to egg extract (Macaulay and Forbes, 1996; Rotem et al., 2009). This type of assembly results in thin, elongated chromatin units of similar dimensions in control and inhibited assembly reactions (Fig. 2B, insets), and in membrane recruitment kinetics that are similar to those observed in solution (data not shown). We chose the 45 minute time point and prepared anchored chromatin assembly reactions for imaging by field emission scanning electron microscopy (FESEM). Both the control and the BAPTA-inhibited chromatin templates were

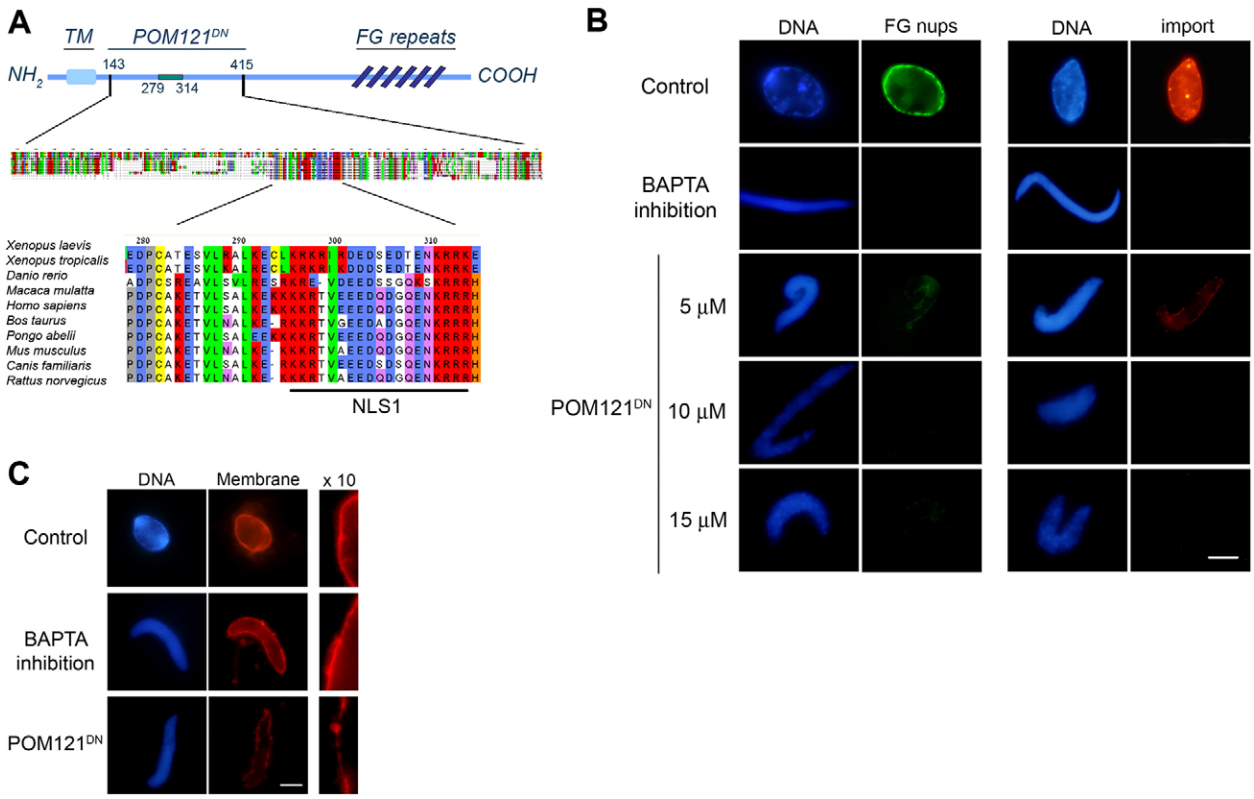

Fig. 1. An internal fragment of POM121 inhibits NPC assembly. (**A**) Schematic representation of *Xenopus* POM121 topology. The internal fragment amino acids 143–415 (POM121^{DN}) is found between the transmembrane segment (TM) and the FG repeat domain. A conserved strip (aa 279–314) within this region is enlarged below. Note the two clusters of basic charges (red) forming the NLS motif. (**B**) Nuclear reconstitution reactions were performed in the presence of 15 μM GST (control), 5 mM BAPTA or increasing amounts of GST-POM121^{DN}. In the control, mAb414 strongly stained mature NPCs and TRITC–NLS–BSA accumulated inside nuclei. BAPTA and POM121^{DN} blocked NPC formation. (**C**) Nuclei were formed in the presence of fluorescently labeled membranes. Control and BAPTA-inhibited nuclei were encompassed by a continuous layer of membranes. Nuclei grown in the presence of 10 μM POM121^{DN} showed irregular and weaker staining, indicating that complete membrane vesicle fusion had not occurred. DNA was stained with Hoechst 33258. Scale bars: 10 μm.

fully enclosed by membranes (Fig. 2B, left and middle panels). Abundant NPCs were present in the control, whereas no NPC-related structures were observed on the smooth membrane surface of BAPTA intermediates. By contrast, anchored chromatin templates assembled in the presence of POM121^{DN} had a very uneven surface (Fig. 2B, right panel) with large areas of exposed chromatin (arrowhead), occasional areas covered with flattened fused membranes (thin arrow) and additional membranes vesicles docked onto chromatin or other membranes (thick arrow). No NPCs were observed in the areas covered by fused membranes. This indicated that nuclear assembly and NPC formation were disrupted by POM121^{DN} at an early stage.

POM121^{DN} is targeted to chromatin

The earliest characterized step in postmitotic NPC assembly is the seeding of chromatin by ELYS and the Nup107–160 nucleoporin complex, which can occur even in the absence of membranes (Rasala et al., 2008). We first investigated whether the recombinant POM121^{DN}–GST fusion protein itself was binding to chromatin and blocking access of the ELYS–Nup107–160 seeding module. Anchored chromatin templates were incubated in membrane-free cytosol and analyzed by immunofluorescence staining. An anti-GST antibody was used to detect the fusion protein, resulting in a strong signal on the surface of chromatin (Fig. 3A). Immunogold staining for FESEM demonstrated the specificity of the anti-GST antibody and also that the POM121^{DN} binding sites are dispersed over the three-dimensional surface of chromatin (supplementary material Fig. S2A). To determine whether chromatin binding by POM121^{DN} prevented seeding, we followed several specific components of the seeding module. Immunoblot analysis of the chromatin-bound fraction demonstrated that ELYS, Nup133 and Nup107 were all recruited to chromatin at normal levels when POM121^{DN} was present in cytosol (Fig. 3B, left). This was confirmed by immunofluorescent staining with an anti-Nup107 antibody (Fig. 3B, right).

Next, we examined whether the binding of recombinant POM121^{DN} to chromatin affected the recruitment of the endogenous full-length POM121 from the membrane fraction to the nuclear periphery. GST or the POM121^{DN} fusion protein were added to the full assembly system containing membranes, and nuclei were separated from cytosol by centrifugation through a sucrose cushion. Immunoblot analysis demonstrated that the amount of full-length POM121 recruited to chromatin was reduced when POM121^{DN} was present in the reaction, whereas gp210 remained unaffected (Fig. 3C).

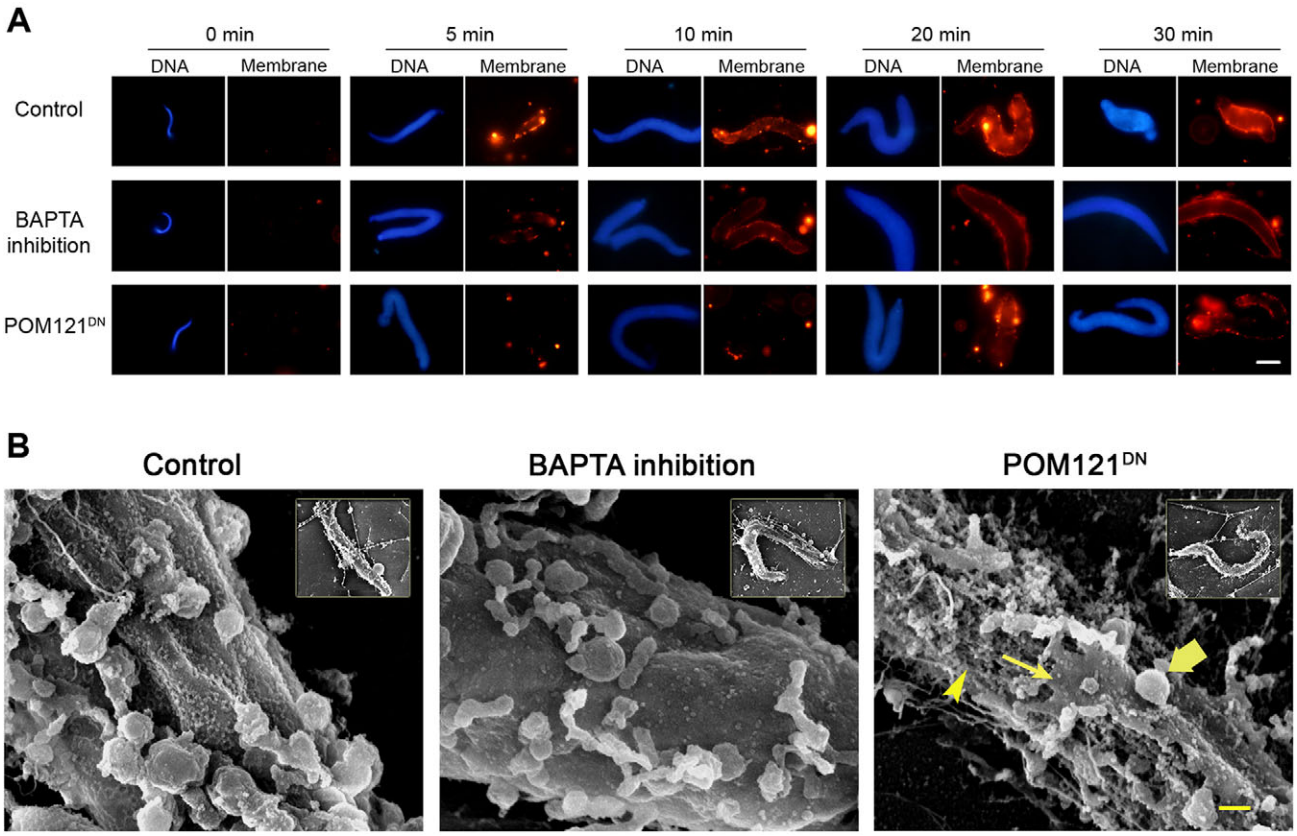

Fig. 2. POM121^{DN} disrupts NE and NPC formation. (**A**) Nuclei were formed in the presence of fluorescently labeled membranes, as in Fig. 1C, and samples were removed for analysis at different time-points. Both control and BAPTA-inhibited assembly reactions showed a steady increase in membrane staining, which resulted in a continuous rim by 20 minutes. Nuclei inhibited by POM121^{DN} showed a substantial delay in the recruitment of membrane vesicles to the surface of chromatin. Scale bar: 10 µm. (**B**) Chromatin templates were pre-attached to silicon chips and incubated in complete reconstitution mixtures containing *Xenopus* egg cytosol and membranes. After 45 minutes of assembly, samples were fixed and prepared for imaging by FESEM. Anchored nuclei in the control reaction were enclosed by a mature NE with abundant NPCs. BAPTA-inhibited nuclei were fully enclosed by smooth membranes with no NPCs. Chromatin templates assembled in the presence of 10 µM POM121^{DN} contained large areas of exposed chromatin (arrowhead), docked membranes vesicles (thick arrow) and some flattened membrane sheets (thin arrow). A region containing examples of all three of these features is shown here. We note, however, that all of the templates we examined had large areas of exposed chromatin. Insets show low magnification images of the anchored templates. Scale bar: 200 nm.

POM121^{DN} and ELYS–Nup107–160 are independently recruited to chromatin

Taken together, our results suggest that the POM121^{DN} fragment exerts its dominant-negative effect by direct binding to chromatin, but this binding does not prevent the seeding of chromatin by ELYS–Nup107–160. Conversely, POM121^{DN} binding might depend on previous seeding by ELYS–Nup107–160. To test this possibility, we immunodepleted ELYS from egg cytosol (supplementary material Fig. S3A) and used the anchored chromatin immunofluorescence assay to follow Nup107 and POM121^{DN}. As expected from previous work (Franz et al., 2007; Rotem et al., 2009), the depletion of ELYS abolished Nup107 binding to chromatin (Fig. 3D, bottom left panels). However, POM121^{DN} still bound strongly to the chromatin periphery, as demonstrated by anti-GST staining (Fig. 3D, right panels). We conclude that POM121^{DN} and ELYS–Nup107–160 are independently recruited to chromatin.

The inhibitory effect of POM121^{DN} is distinct from the results of immunodepletion

Previous work in the *Xenopus* assembly system by Antonin and colleagues has led to the suggestion that POM121 coordinates NPC assembly with NE fusion (Antonin et al., 2005). In that study, immunodepletion of POM121-containing membrane vesicles, or solubilization of the membranes followed by immunodepletion of the protein itself, prevented the formation of a continuous NE. This phenotype is similar to that observed after the addition of the POM121^{DN} fragment in our experiments (Figs 1, 2). Surprisingly, Antonin et al. also found that co-depletion of the Nup107–160 complex and POM121 suppressed the inhibitory effect on membranes, leading to a fully enclosed NE, albeit with no NPCs (Antonin et al., 2005). We therefore investigated whether depletion of the ELYS–Nup107–160 seeding module would 'rescue' NE sealing when nuclear assembly is conducted in the presence of POM121^{DN}. Mock-depleted and ELYS-depleted cytosol were used in reconstitution reactions containing chromatin and fluorescently labeled membranes, with or without the addition of the POM121^{DN} fragment. Both of the control reactions showed a continuous membrane staining pattern at the nuclear periphery (supplementary material Fig. S3B, left). The addition of POM121^{DN} inhibited the formation of a continuous NE and this effect was not reversed by the depletion of ELYS–Nup107–160 (supplementary material Fig. S3B, bottom right). Thus, the

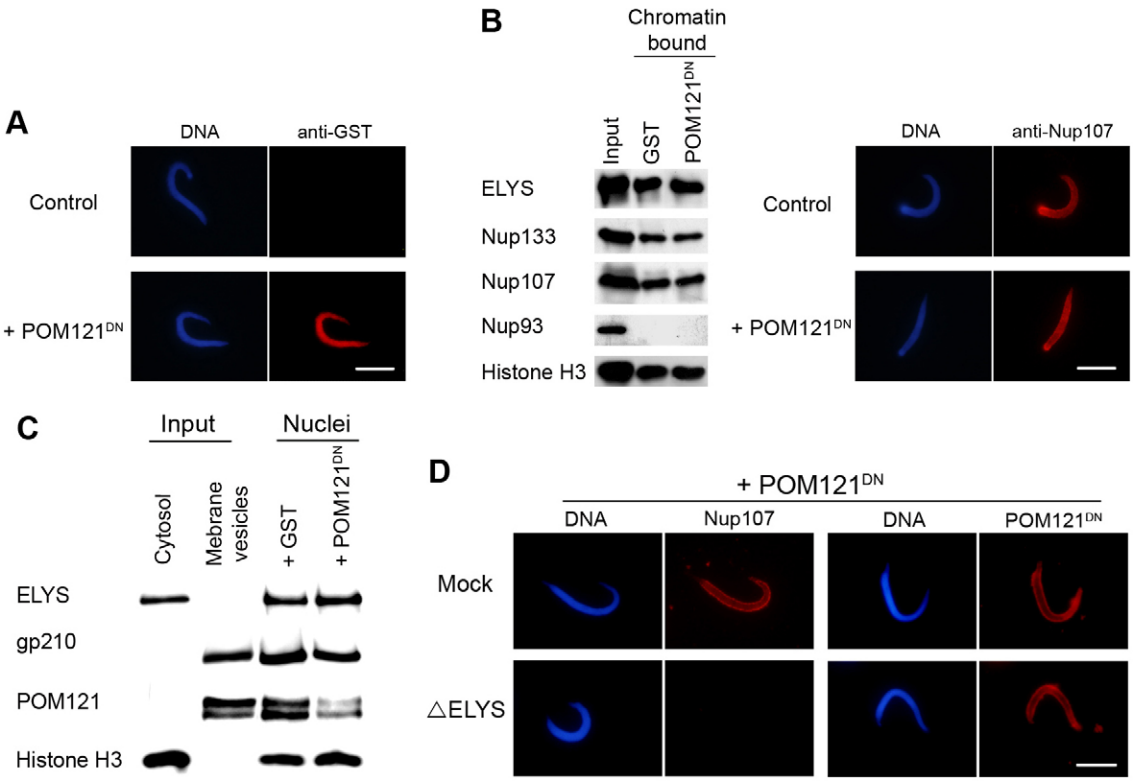

Fig. 3. POM121^{DN} and ELYS–Nup107–160 are independently recruited to chromatin. (**A**) Anchored chromatin binding assays were conducted with membrane-free cytosol supplemented with 10 μM GST or POM121^{DN} and processed for indirect immunofluorescence. Anti-GST staining was used to check the localization of the recombinant proteins added into cytosol: GST was present in the control reaction but did not stain chromatin, whereas the POM121^{DN} fusion protein produced a strong signal on chromatin. (**B**) Anchored chromatin binding assays were set up with GST (control) or POM121^{DN} as in A. The chromatin-bound fraction was analyzed by immunoblotting with antibodies directed against ELYS, Nup133 and Nup107 (members of the chromatin seeding complex), Nup93 (a nucleoporin that is not targeted to chromatin in the absence of membranes) and histone H3. Immunofluorescent staining with anti-Nup107 produced a strong signal on chromatin under both conditions, confirming that seeding had occurred. (**C**) Full assembly reactions were incubated with 10 μM GST or POM121^{DN} for 30 minutes and then spun through sucrose cushions. ELYS and histone H3 were recovered in the nuclear fraction and served as controls. The amount of endogenous POM121 recruited to the nuclear fraction was reduced in the presence of POM121^{DN}, whereas gp210 was unaffected. (**D**) Mock-depleted and ELYS-depleted egg cytosol were compared in the chromatin binding assay. Anti-Nup107 staining confirmed that the depletion of ELYS prevented chromatin seeding by ELYS–Nup107–160. However, POM121^{DN} still bound to chromatin in the absence of the seeding complex. Scale bars: 10 μm.

inhibitory effect of the POM121^{DN} fragment is distinct from the effects of immunodepleting the endogenous membrane protein. In addition, the overall distribution of POM121^{DN} on the three-dimensional surface of chromatin remained unchanged when ELYS was depleted from cytosol and chromatin seeding was inhibited (supplementary material Fig. S2B).

Importin-β negatively regulates the chromatin binding determinants of POM121 and ELYS–Nup107–160

We and others have previously shown that importin-β negatively regulates several distinct steps in postmitotic NPC assembly, including chromatin seeding by ELYS–Nup107–160 (Harel et al., 2003a; Lau et al., 2009; Rotem et al., 2009; Walther et al., 2003). We next investigated whether importin-β was also capable of regulating the binding of POM121^{DN} to chromatin. Indeed, the addition of excess importin-β into cytosol prevented POM121^{DN} binding in both the immunoblot and immunofluorescence anchored-chromatin assays (Fig. 4A,B). The binding of the recombinant POM121 fragment to chromatin was more sensitive to this negative regulation by importin-β than the binding of the endogenous ELYS–Nup107–160 complex (Fig. 4A). The inhibitory effect of importin-β was readily reversed by an excess of the RanQ69L mutant, which is locked in the GTP-bound form, and this was quantified in the immunofluorescence binding assay (Fig. 4B). A comparison of the immunofluorescence signals in this assay indicated that importin-β was able to reduce POM121^{DN} binding by ~88% and an excess of RanQ69L–GTP returned binding to the initial levels (Fig. 4B, right). Thus, under physiological conditions, the high concentration of RanGTP near the surface of chromatin would be expected to tip the regulatory balance towards POM121 binding. These results suggest that importin-β regulates two independent chromatin binding modules: the membrane-anchored POM121 and the soluble ELYS–Nup107–160 complex (see Discussion).

Importin-β negatively regulates the recruitment of endogenous POM121 at an early stage of assembly

To determine whether the negative regulatory effect of importin-β on POM121^{DN} binding reflects its interactions with the endogenous membrane protein, we decided to re-investigate the effect of adding excess importin-β to the full assembly system (Harel et al., 2003a). We used fluorescently labeled membranes to follow vesicle targeting and fusion on the surface of chromatin and two specific antibodies to follow POM121 and gp210

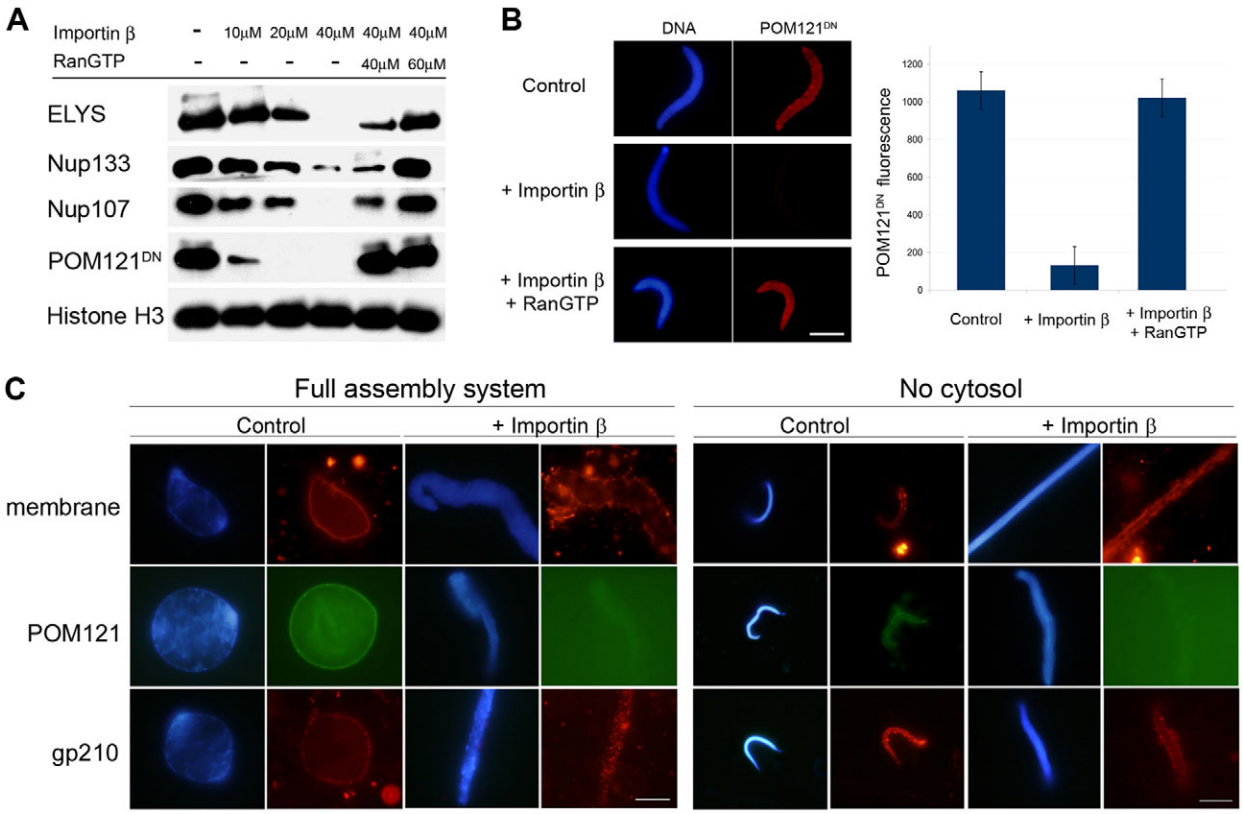

Fig. 4. Importin-β negatively regulates the binding of POM121^{DN} to chromatin. Anchored chromatin binding assays were conducted as in Fig. 3. (**A**) Immunoblot analysis of the chromatin-bound fraction in reactions containing different amounts of importin-β and RanGTP. Increasing amounts of importin-β reduced the binding of the ELYS–Nup107–160 complex members and of the POM121^{DN} fragment to chromatin. An excess of RanQ69L–GTP over importin-β restored binding. Histone H3 served as a loading control. (**B**) POM121^{DN} was incubated in cytosol at 3 μM and the effect of 40 μM importin-β or a combination of 40 μM importin-β and 60 μM RanGTP, on chromatin binding was tested. Representative single chromatin templates stained with anti-GST are shown on the left and a quantitative analysis of multiple templates in two independent experiments is shown on the right. See Materials and Methods for details. Error bars indicate the standard deviation (s.d.). (**C**) Untagged *Xenopus* importin-β was added at 20 μM to full assembly reactions (left), or assembly mixtures in which cytosol was replaced with 5% BSA–ELB (right). Fluorescently labeled membranes were used as in Fig. 1C. Anti-POM121 and anti-gp210 were used to follow specific membrane components. Excess importin-β caused a reduction in POM121 staining on the surface of chromatin in the full assembly mixture as well as in the cytosol-free reaction. Scale bars: 10 μm.

(Fig. 4C). As previously reported, excess importin-β blocked nuclear assembly at an early stage and resulted in docked, unfused membrane vesicles, visualized by a general membrane dye. Anti-POM121 staining revealed that the endogenous membrane protein was strongly affected by importin-β and did not appear to be substantially recruited to the surface of chromatin. By contrast, anti-gp210 clearly stained membrane vesicles on the surface of these aborted assembly intermediates (Fig. 4C, left, +importin-β columns). Very similar results were obtained when cytosol was omitted from the assembly reactions (Fig. 4C, right), supporting the notion that endogenous POM121 has an intrinsic capability to be targeted to chromatin and that this targeting is regulated by importin-β.

The conserved NLS within POM121^{DN} mediates the regulatory effect of importin-β

Our results suggest a complex regulatory interplay between importin-β, RanGTP and POM121, which are all targeted to chromatin at the exit from mitosis. Recent work by two groups (Doucet et al., 2010; Yavuz et al., 2010) has pointed to two classical bipartite NLS motifs in the central region of *Xenopus laevis* POM121 as the crucial determinants for interaction with importin-β. One of these bipartite NLSs, designated NLS1 by Yavuz et al. is present within the POM121^{DN} fragment as part of a highly conserved 35 amino acid strip (Fig. 1A) (Yavuz et al., 2010). A possible interpretation of our data might be that the crucial determinants for POM121^{DN} action are all present within this conserved strip and that in vivo, importin-β modulates the targeting of the full length membrane-anchored POM121 by masking this region.

To investigate the functional role of the NLS1 motif, we first examined whether the POM121^{DN} fragment could affect the function of NPCs after their assembly. Nuclei were assembled for 1 hour and the recombinant fragment was then added and incubated in the assembly reaction. Mature NEs with functional NPCs were formed, as determined from the normal rim staining by mAb414 and the accumulation of the M9–GFP cargo, imported by transportin (Fig. 5, FG Nups and M9-GFP import). However, a classical NLS–BSA cargo was excluded from the nuclei to which POM121^{DN} was added at this late time point (Fig. 5, second row). This suggests a specific perturbation of the importin-α/β pathway. Next, we focused on the conserved

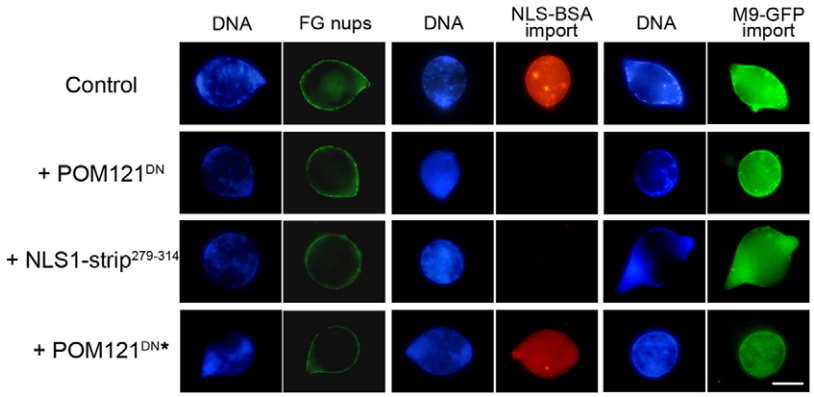

Fig. 5. POM121^{DN} affects the classical import pathway through the conserved NLS motif. Normal nuclei were assembled for 1 hour before the addition of 10 µM GST, 10 µM POM121^{DN}, 20 µM NLS1-strip$^{279–314}$ or 10 µM POM121^{DN*} and the incubation continued for a further 20 minutes, followed by import assays or staining with mAb414. All nuclei showed normal rim staining by mAb414 and transportin-mediated import of M9–GFP. The addition of POM121^{DN} or the smaller NLS1-strip$^{279–314}$ specifically blocked the importin-α/β pathway. POM121^{DN*}, with the inactivated NLS1 motif, had no effect on import in pre-assembled nuclei. Scale bar: 10 µm.

35-amino-acid strip containing the NLS motif, and expressed it in a soluble recombinant form. When this NLS1-strip$^{279–314}$ was added to nuclear reconstitution reactions after nuclei had assembled, it also blocked the importin-α/β pathway (Fig. 5, third row). When NLS1-strip$^{279–314}$ was added at $t=0$, it specifically blocked importin-β-mediated import, but it was not sufficient to inhibit NE and NPC assembly (supplementary material Fig. S4A). Thus, the conserved NLS strip appears to mediate the importin-β-interactions of POM121^{DN}, but does not account in itself for the dominant-negative effect on NPC assembly.

POM121^{DN} with an inactivated NLS is still a potent inhibitor of nuclear assembly

Based on our findings with the NLS1-strip, we predicted that inactivating the NLS motif in POM121^{DN} would abolish the interaction with importin-β, but not the inhibitory effect on NE and NPC assembly. We generated point mutations in the bipartite NLS (supplementary material Fig. S4B) and tested the resulting POM121^{DN*} fragment in an import assay with pre-assembled nuclei. As expected, the recombinant fragment with a mutated NLS no longer blocked the importin-α/β pathway (Fig. 5, compare second and fourth rows). Next, we tested both the original and mutated recombinant fragments for their effect on nuclear assembly in reconstitution reactions containing fluorescently labeled membrane vesicles. Both POM121^{DN} and POM121^{DN*} prevented the formation of a continuous NE (Fig. 6A). Staining with mAb414 and import assays confirmed that no NPCs were formed in these reconstitution reactions (data not shown). We next tested the ability of the POM121^{DN*} fragment to bind chromatin in the anchored chromatin assay. POM121^{DN*} produced a specific staining pattern on the surface of chromatin and this binding was insensitive to the addition of excess importin-β (Fig. 6B). We conclude that the POM121^{DN*} protein, containing the inactivated NLS, still binds chromatin and is a potent inhibitor of NE and NPC assembly in the postmitotic mode. Lastly, we tested the localization of POM121^{DN} and POM121^{DN*} when added after the assembly of functional nuclei and NPCs. The POM121^{DN} fragment strongly accumulated inside the nucleoplasm, whereas POM121^{DN*} was not targeted to pre-assembled nuclei (Fig. 6C). Thus, NLS-mediated entry through existing NPCs and chromatin binding are two separate functions, although they map to the same region of POM121.

The analysis of nine different internal fragments of *Xenopus* POM121 in the anchored chromatin binding assay is summarized

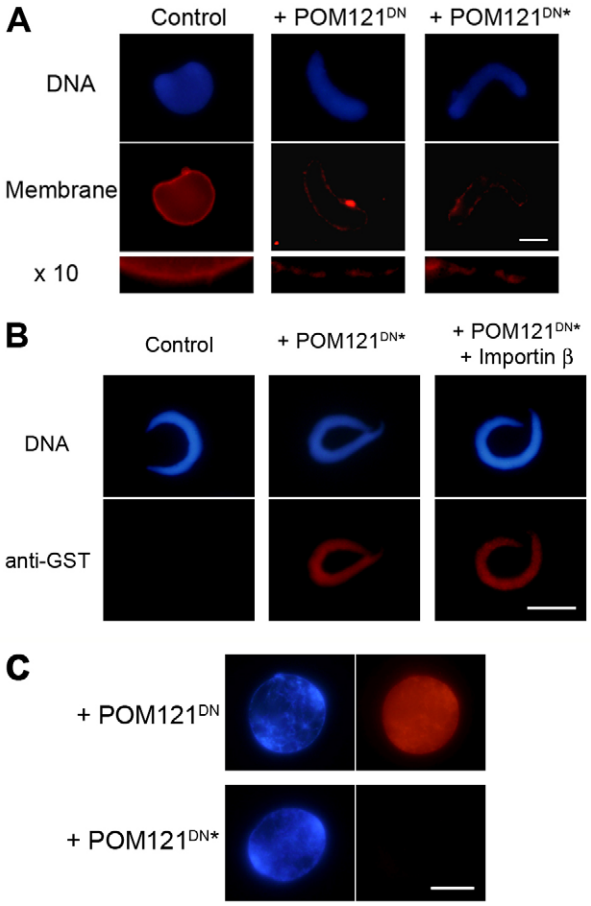

Fig. 6. POM121^{DN*} inhibits nuclear assembly and is insensitive to regulation by importin-β. (**A**) Nuclear reconstitution was performed with fluorescently labeled membranes and the addition of 10 µM GST (control), 10 µM POM121^{DN} or 10 µM POM121^{DN*}. Strong, continuous membrane staining encircled the control nuclei, whereas a weaker irregular staining was observed in the presence of both POM121 fragments. (**B**) Anchored chromatin binding assays were conducted with membrane-free cytosol as in Fig. 4B. POM121^{DN*} was added to cytosol at 3 µM and produced a specific signal on chromatin, which was not diminished by an excess of 40 µM importin-β. (**C**) Fluorescently labeled POM121^{DN} or POM121^{DN*} were added at 20 nM to nuclear reconstitution reactions after 1 hour of assembly. Only POM121^{DN} accumulated inside the pre-assembled nuclei. Scale bars: 10 µm.

in supplementary material Fig. S5. This analysis suggests that the chromatin binding activity of the POM121^{DN} fragment results from the combined effect of at least two separate regions flanking the NLS1 motif. These putative chromatin binding elements are not immediately adjacent to the NLS itself and do not overlap the conserved 35 amino acid strip containing this motif (see Discussion).

POM121^{DN} prevents nuclear membrane expansion in the interphase assembly mode

To determine whether the POM121^{DN} fragment can also perturb the interphase mode of NPC assembly, we used the inhibition-and-rescue approach in the *Xenopus* reconstitution system (Harel et al., 2003a) (see also D'Angelo et al., 2006). Fully sealed, poreless NEs were first assembled in the presence of 5 mM BAPTA, and inhibition was subsequently relieved by dilution in fresh cytosol (Fig. 7A, control). Rescued nuclei were round and contained decondensed chromatin and functional NPCs, as determined by mAb414 staining and import assays (Fig. 7A, middle panels). Because NPCs are inserted into pre-existing double nuclear membranes in this scenario, we could identify whether the soluble POM121^{DN} fragment affected assembly under interphase settings. When POM121^{DN} was added to cytosol in the rescue phase (following 1 hour of assembly in the presence of BAPTA), chromatin remained condensed and the NE did not expand (Fig. 7A, right). However, these rescued intermediates stained strongly with mAb414 and contained at least some functional NPCs, because M9–GFP import was restored (Fig. 7A, bottom right).

The observed inhibitory effect of POM121^{DN} in this experiment can be interpreted in different ways. The initial insertion of functional NPCs into the sealed nuclear membranes might allow access and binding of the dominant-negative fragment to chromatin and thus prevent chromatin decondensation. The POM121^{DN} fragment might also be acting at the membrane level by preventing further recruitment of membrane components, thus blocking nuclear membrane expansion.

To test for a potential effect on the membranes, we first assembled normal nuclei for 1 hour and subsequently added the recombinant proteins. We then monitored the expansion of the NE upon continued incubation in egg extract. All of the nuclei were round and contained decondensed chromatin (Fig. 7B). The average surface area of nuclei in the control reaction was nearly doubled during the second hour of incubation and continued to increase within the third hour (Fig. 7B, top row and +GST histograms). By contrast, the addition of the POM121^{DN} fragment effectively blocked all further expansion of the NE (Fig. 7B, middle row and +POM121^{DN} histograms).

This dramatic effect on nuclear expansion could theoretically be attributed to the specific blocking of the importin-α/β pathway by POM121^{DN}. A recent study has demonstrated that nuclear size is strongly correlated to titratable factors in *Xenopus* egg extracts,

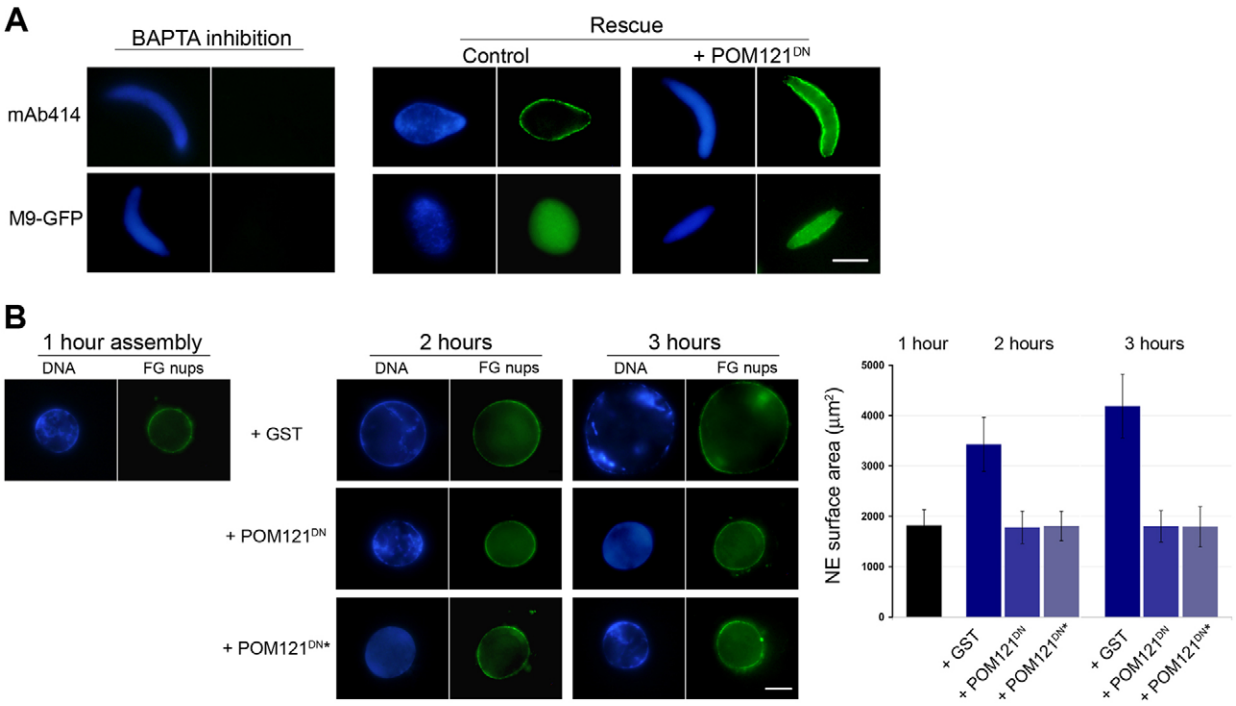

Fig. 7. POM121^{DN} blocks NE expansion in the interphase assembly mode. (**A**) Nuclear reconstitution of poreless NEs was performed by incubation with 5 mM BAPTA as in Figs 1, 2. Complete inhibition of NPC formation was confirmed by the lack of mAb414 staining and failure in M9–GFP import (left panels). Rescue from BAPTA inhibition was achieved by dilution in fresh cytosol containing 10 μM GST or POM121^{DN}. Rescued nuclei in the control had decondensed chromatin, accumulated M9–GFP and showed punctate rim staining by mAb414 (middle panels). By contrast, rescue in the presence of POM121^{DN} resulted in elongated nuclei with condensed chromatin and a consistently stronger mAb414 immunofluorescence signal. M9–GFP import was restored in these nuclei (right panels). (**B**) To monitor NE expansion in the interphase mode, nuclei were assembled for 1 hour, followed by the addition of 10 μM GST, 10 μM POM121^{DN} or 10 μM POM121^{DN*}. Samples were removed and fixed 1 or 2 hours after further incubation and stained with Hoechst 33258 and mAb414. Representative nuclei are shown. The NE surface area of 30 randomly chosen nuclei in each category was quantified, as summarized in the histograms on the right. NE expansion was completely blocked in the presence of POM121^{DN} or POM121^{DN*}. Error bars indicate the s.d. Scale bars: 10 μm.

namely importin-α, which is responsible for the rate of import of lamin B3 (Levy and Heald, 2010). To investigate whether the observed block in NE expansion was due to perturbation of the importin-α/β pathway, we tested the effect of the mutated POM121^{DN*} fragment on pre-assembled nuclei (Fig. 7B, bottom row and +POM121^{DN*} histograms). The fragment with the inactivated NLS had an identical effect to the POM121^{DN} fragment and blocked all further expansion of the NE. The addition of the smaller NLS1-strip$^{279–314}$ fragment decreased the rate of nuclear growth, but did not block NE expansion altogether (supplementary material Fig. S6). Thus, the dominant-negative POM121^{DN} fragment completely blocks NE expansion in the interphase assembly mode and does so independently from the NLS-mediated interaction with importin-α and importin-β.

The block in membrane expansion results in densely packed NPCs

The results of mAb414 staining (Fig. 7A,B) suggest that new NPCs were inserted into a pre-existing NE in the presence of POM121^{DN}, but further expansion of the membranes was inhibited. To directly visualize the results of the inhibition of membrane expansion in the interphase assembly mode, we prepared samples for imaging by FESEM. Normal assembly was carried out for the minimum time required to form an enclosed envelope. GST or POM121^{DN} were then added and the assembly reactions were further incubated to allow NPC insertion into the intact NEs. Mature NPCs were dispersed over the surface of control nuclei with plenty of exposed membrane areas in the intervening spaces (Fig. 8, control). By contrast, densely packed NPCs covered the entire surface of nuclei assembled in the presence of POM121^{DN}, with only minimal exposed nuclear membranes in between (Fig. 8, right). Morphometric analysis of comparable areas of flat NE showed a large difference in the average density of NPCs in such experiments (Fig. 8, histograms).

In summary, the POM121^{DN} fragment has a dominant-negative effect on both modes of assembly in the cell-free reconstitution system. The addition of this soluble fragment of POM121 uncouples NE formation or expansion from NPC assembly and results in two drastically different and abnormal phenotypes. This suggests that POM121 plays an important mechanistic role in both the postmitotic and interphase modes of NPC assembly.

Discussion

In this study, we used the *Xenopus* nuclear reconstitution system to investigate the role of POM121 in nuclear pore and NE assembly. We describe the dominant-negative effects of a soluble POM121 fragment on both the postmitotic and interphase modes of assembly. The region of *Xenopus* POM121 that contains the dominant-negative fragment has been previously implicated in forming interactions with importin-α and importin-β and some nucleoporins (Rasala et al., 2008; Yavuz et al., 2010). A similar internal domain of human POM121 induces the ectopic recruitment of soluble Nups to mitochondria, when targeted to the outer mitochondrial membrane (Stavru et al., 2006b). Recent work has identified direct interactions of the same general region of human POM121 with the β-propeller domains of Nup160 and Nup155 (Mitchell et al., 2010). It is therefore logical to assume that our POM121^{DN} fragment contains binding elements that participate in the Nup–Nup interactions that build up the NPC. However, our results also point to other important interactions mediated by this domain (Fig. 9).

The strongest inhibitory effect of the soluble POM121^{DN} fragment is observed in the postmitotic mode, when it is added to nuclear reconstitution reactions at $t=0$. The POM121^{DN} fragment is targeted to the surface of chromatin and disrupts membrane recruitment, preventing the formation of a continuous NE. FESEM analysis reveals large areas of exposed chromatin and only partial enclosure by membranes, with no sign of NPCs (Fig. 2B). These observations are in good agreement with the previously reported results of immunodepleting POM121- or NDC1-containing vesicles from egg extract (Antonin et al., 2005; Mansfeld et al., 2006). Several distinct subpopulations of membrane vesicles have been described in *Xenopus* egg extracts that differ in their ability to bind chromatin and fuse to other membranes (Antonin et al., 2005; Drummond et al., 1999; Sasagawa et al., 1999; Vigers and Lohka, 1991). Our results show that both the dominant-negative fragment and excess importin-β reduce the amount of endogenous POM121 that is targeted to chromatin, but do not affect gp210 (Fig. 3C, Fig. 4C). This is consistent with a block in the recruitment of membrane vesicles that are enriched in POM121 and NDC1 (Antonin et al., 2005). Importantly, the presence of the POM121^{DN} fragment is also sufficient to block FG Nup recruitment (as determined by

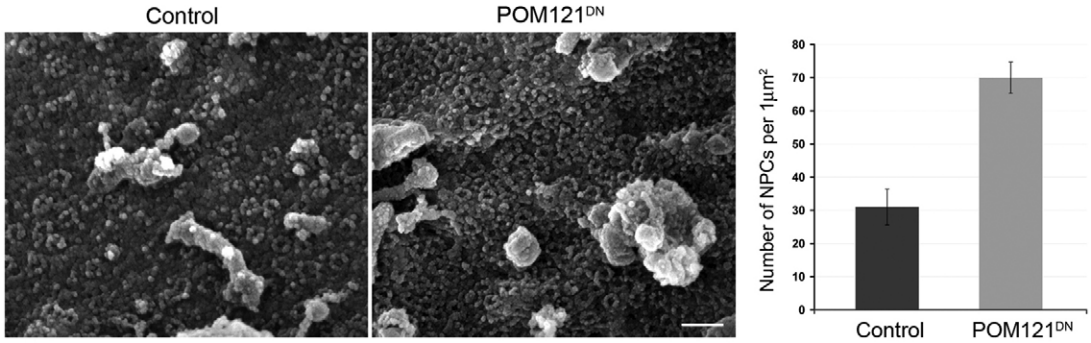

Fig. 8. The block in NE expansion results in densely packed NPCs with no exposed membrane. Nuclear reconstitution reactions were incubated for 30 minutes at room temperature to ensure that chromatin was fully enclosed in membranes and NPC assembly had commenced. Reactions were then supplemented with 10 µM GST or POM121^{DN} and incubated for a further 40 minutes. Samples were spun onto silicon chips, fixed and prepared for FESEM. Control nuclei had typical mature NEs, with NPCs interspersed with clearly visible patches of nuclear membrane surface (left). Nuclei assembled in the presence of POM121^{DN} were densely covered with NPCs, with minimal exposure of membrane surface (right). The effect of POM121^{DN} on NPC density was quantified in two separate experiments (histograms). Scale bar: 300 nm.

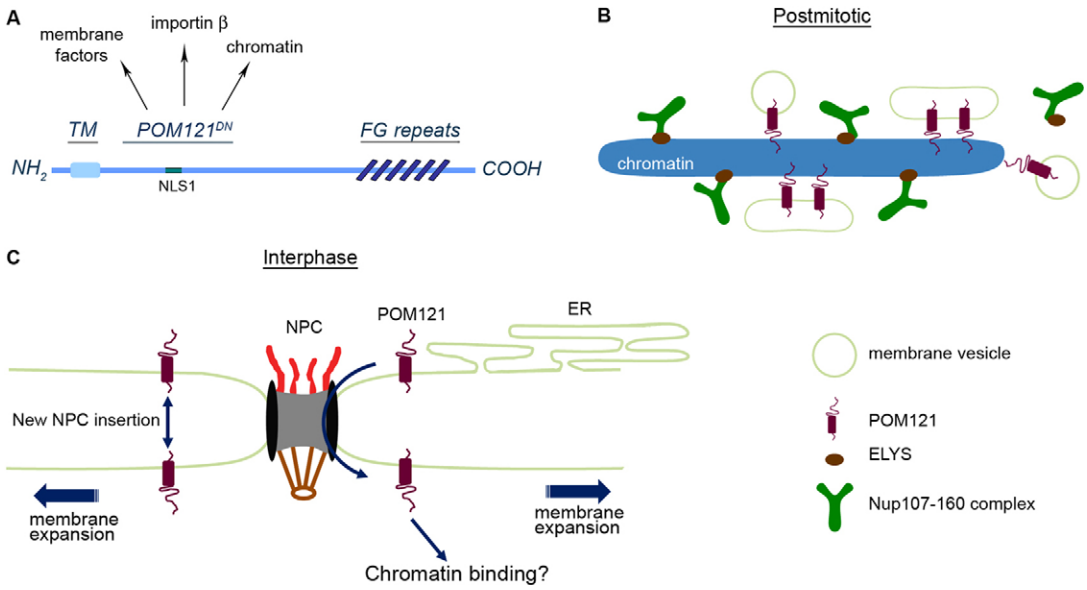

Fig. 9. Model for POM121 function in NPC assembly. (**A**) Different types of interactions converge on the internal POM121^{DN} segment. The dominant-negative effect of this soluble fragment in the cell-free reconstitution system is seen as a partial block in membrane enclosure and complete inhibition of NPC assembly. In the interphase assembly mode, NPCs are inserted into the intact NE, but membrane expansion is inhibited. (**B**) The earliest step in postmitotic NPC assembly involves the independent recruitment of POM121 and ELYS–Nup107–160 to chromatin. Both of these chromatin-targeting events are negatively regulated by importin-β. (**C**) During interphase, additional POM121 molecules are targeted through existing NPCs to the inner nuclear membrane. New NPC assembly proceeds through interactions between the inner and outer nuclear membrane and is coordinated with continued membrane expansion. The soluble POM121^{DN} fragment uncouples NPC formation from membrane expansion, without the need to enter the nucleoplasm.

mAb414 staining) and the formation of NPC-related structures (identified by FESEM) in the postmitotic mode of assembly.

These results suggest that the central domain of POM121 is involved in three important functions: (1) targeting to chromatin; (2) soluble Nup recruitment; and (3) the completion of nuclear membrane assembly. Antonin et al. have previously suggested that POM121 is an essential component of a checkpoint mechanism that coordinates early steps in NPC assembly with fusion events required for NE formation (Antonin et al., 2005). Our current results support this view of a functional link between NE and NPC assembly, although it is not necessary to regard this as a true cell-cycle-dependent checkpoint mechanism (Stavru et al., 2006a). Interestingly, our results differ from those of the depletion of POM121 from membranes, in that co-depletion of ELYS–Nup107–160 does not 'rescue' the formation of a continuous NE. This suggests that the blocking of chromatin attachment sites by POM121^{DN} is a major facet of the dominant-negative effect, and implies that other membrane proteins might provide the chromatin targeting function when POM121 is absent.

Our results show that POM121^{DN} binds to chromatin and prevents its enclosure by a continuous NE. This inhibitory effect is specific, because 'seeding' by ELYS–Nup107–160 is not affected. Previous studies have implicated multiple integral membrane proteins, including POM121, in direct binding to chromatin (Anderson et al., 2009; Ulbert et al., 2006). However, these interactions have been generally assumed to be collaborative and redundant. Our observations suggest that POM121^{DN} binds to specific sites on chromatin, which are essential for nuclear assembly, but are distinct from the ELYS binding sites. We mapped the chromatin binding elements within the POM121^{DN} fragment to two separate regions flanking the NLS1 motif, but not immediately adjacent to it. These regions are not well conserved in vertebrates and do not contain any known DNA binding or other motifs. To date, no specific DNA sequences have been implicated in the targeting of any nucleoporin to chromatin, although the chromatin binding elements in ELYS have been identified as an AT-hook motif and one additional region (Rasala et al., 2008). Thus, an important future challenge will be to define the precise molecular interactions, either protein–protein or protein–DNA, that initiate postmitotic NPC assembly on chromatin.

Our data indicate that POM121 and ELYS–Nup107–160 are independently recruited to chromatin in the postmitotic assembly mode. Strikingly, both of these chromatin-binding modules are negatively regulated by importin-β. This explains the previously reported inhibition of membrane vesicle fusion by excess importin-β (Harel et al., 2003a). Because the regulatory interaction between importin-β and POM121 can be reproduced in the absence of cytosl, our results also support the existence of a membrane-associated sub-population of importin-α (Hachet et al., 2004). Recent work has identified five functional NLS motifs in the same general region of one of the human POM121 genes and suggests that these are essential for targeting the protein to the inner nuclear membrane during interphase (Funakoshi et al., 2011). Pulldown experiments performed by Yavuz et al. with different fragments of *Xenopus* POM121 suggest that the two bipartite NLSs of the *Xenopus* protein form strong interactions with importin-α. Importin-α in turn, mediates RanGTP-sensitive interactions with importin-β and FG Nups (Yavuz et al., 2010). This is in good agreement with our results, showing that inhibition by importin-β of chromatin binding by POM121^{DN} is readily reversed by RanGTP. However, our results also show that the POM121^{DN*} fragment, possessing an inactivated NLS, is still

a potent inhibitor of NE and NPC assembly. This indicates that the dominant-negative effects of POM121^{DN} on assembly are not the result of NLS-mediated interactions.

We suggest that in the postmitotic assembly mode the NLS1 motif of POM121 provides a means for regulating the rate of membrane recruitment to the surface of chromatin. Our findings do not exclude the possibility that the POM121 NLSs might play a separate, import-related function in interphase assembly (Doucet et al., 2010; Funakoshi et al., 2011; Yavuz et al., 2010) (see also Fig. 9C). Although ELYS–Nup107–160 was previously suggested to recruit POM121 to chromatin (Rasala et al., 2008), we now show that both of these modules need to bind chromatin before postmitotic NPC assembly can commence (Fig. 9B). The interaction of POM121 with Nup160 (Mitchell et al., 2010), is likely to represent a subsequent step in the assembly process, which might be required to induce fusion of the inner and outer nuclear membrane and the formation of an initial pore channel (Fichtman et al., 2010).

The POM121^{DN} fragment also interferes with NPC insertion into intact membranes in the in vitro assembly system (Figs 7, 8). These experimental conditions serve as a model for the interphase mode of assembly in metazoan cells (D'Angelo et al., 2006; Doucet et al., 2010; Harel et al., 2003a; Vollmar et al., 2009). When POM121^{DN} is added to a pre-formed NE, NPC insertion does occur, but it is uncoupled from nuclear membrane expansion. Direct visualization by FESEM reveals densely packed NPCs with very minimal patches of exposed nuclear membrane surface. This is somewhat reminiscent of the phenomenon of 'NPC clustering', reported in yeast (Doye and Hurt, 1997; Gorsch et al., 1995; Heath et al., 1995; Pemberton et al., 1995; Siniossoglou et al., 1996; Wente and Blobel, 1994). This term usually refers to the formation of tight clusters of NPCs interspersed with open stretches of poreless membranes. A similar phenotype is observed in the combined deletion of the yeast reticulon RTN1 and YOP1, both suggested to be ER membrane-bending proteins and implicated in NPC assembly (Dawson et al., 2009). We observe an extreme clustering effect, in the sense that it extends across the whole NE and appears to result from a complete block in membrane expansion. Importantly, the dominant-negative fragment does not need to be localized to the nucleus to exert this effect (Fig. 6C, Fig. 7). We hypothesize that the soluble POM121 fragment competes with the endogenous protein by forming specific protein–protein interactions with membrane assembly factors. These might include membrane-associated proteins such as reticulons, or soluble components of the cytosol (Dawson et al., 2009; Rafikova et al., 2009).

Doucet et al. have recently proposed that POM121 plays a rate-limiting role only in interphase NPC assembly. These authors go on to suggest that NPCs are assembled by two different mechanisms during interphase and at the end of mitosis (Doucet et al., 2010). We believe this conclusion could be premature. Our results point to a distinct and crucial role for POM121 in postmitotic NPC assembly, at least in the *Xenopus* nuclear reconstitution system. Although we describe a very different dominant-negative phenotype in the interphase assembly mode, this might be due to the obvious differences in membrane topology between the two conditions. Little is known about the assembly steps that follow ELYS–107–160 and POM121 recruitment. Thus, it remains possible that NPC assembly per se, is brought about by the same mechanism in the two different cell cycle phases. The data reported here provide support to this view, by demonstrating that NPC biogenesis is intimately linked through POM121 to nuclear membrane formation and/or expansion in both of the assembly modes.

Materials and Methods

Antibodies

Commercially obtained antibodies included rabbit polyclonal anti-GST (ab9085; Abcam), rabbit polyclonal anti-histone H3 (ab1791; Abcam), fluorescently labeled monoclonal Ab414 (A488-120L; Covance), Alexa Fluor 568 goat anti-rabbit (Invitrogen) and 12 nm gold-conjugated goat anti-rabbit (Jackson ImmunoResearch). Previously described, affinity purified antibodies included anti-human-Nup133, anti-*Xenopus*-ELYS and anti-*Xenopus*-Nup107 (Rotem et al., 2009), anti-hNup93, anti-*Xenopus* gp210 and anti-*Xenopus*-POM121 (Harel et al., 2003a; Harel et al., 2003b). A second polyclonal anti-*Xenopus*-POM121 (Antonin et al., 2005), directed against a different region of the protein, was a gift from Wolfram Antonin (Friedrich Miescher Laboratory of the Max Planck Society, Tübingen, Germany).

Recombinant protein expression and purification

Amino acid positions in the full-length coding sequence of *X. laevis* POM121 are those of GenBank accession number AY676874 (Antonin et al., 2005). Coding sequences for the different constructs were inserted into pGEX6P-3 and expressed as GST fusion proteins in the *Escherichia coli* strain BL21 (DE3) RIL. Fusion proteins were purified in the presence of a protease inhibitor cocktail (#11-836-156-001; Roche) on glutathione–Sepharose 4B beads (GE Healthcare), followed by size-exclusion chromatography on a Superdex GL 10/300 S200 column (GE Healthcare). The conserved strip of aa 279-314, containing the bipartite NLS motif, was cloned into a modified zz-pET28 vector (Vasu et al., 2001) to produce a combined zz-histidine-tagged protein. A zz-6xHis-T7-tag control protein was also purified, for comparison. Point mutations in the NLS1 motif of the POM121^{DN} construct were generated by site-directed mutagenesis (QuikChange II; Stratagene). Full-length histidine-tagged human importin-β was expressed and purified as previously described (Harel et al., 2003a). In some experiments untagged *Xenopus* importin-β was tested and produced identical results to the human protein (see Rotem et al., 2009). Expression, purification and loading of RanQ69L with GTP were performed as previously described (Rotem et al., 2009). The histidine-tagged M9–GFP construct was a gift from Michael Elbaum and was expressed and purified as described by Lachish-Zalait et al. (Lachish-Zalait et al., 2009).

Egg extracts, immunodepletion and nuclear reconstitution

Preparation of demembranated sperm chromatin, *Xenopus* egg extracts and separation into cytosolic and membrane fractions were performed as previously described (Harel et al., 2003a). Membrane-free cytosol was prepared by a 1:1 dilution in ELBS (10 mM Hepes pH 7.6, 250 mM sucrose, 50 mM KCl, 2.5 mM $MgCl_2$) and subsequent centrifugation, as previously described (Rotem et al., 2009). For the immunodepletion of ELYS from cytosol, 180 µg of affinity purified anti-ELYS or preimmune IgG were bound to 40 µl of protein A–Sepharose beads (GE Healthcare) and used for two consecutive rounds of depletion, as described by Rotem et al. (Rotem et al., 2009). Nuclei were reconstituted by mixing *Xenopus* egg membrane vesicles and cytosolic fractions at a 1:20 ratio, with an ATP regeneration system, 5 µg/ml nocodazole and sperm chromatin at room temperature (Harel et al., 2003a; Macaulay and Forbes, 1996). Recombinant proteins in ELBS were added at equal concentrations for each set of reactions, with the total volume of addition not exceeding 15% of the reaction.

Functional assays, BAPTA rescue and membrane expansion assay

Pre-labeled fluorescent membranes were prepared essentially as previously described (Hetzer et al., 2000), using CM-DiI (Molecular Probes), and were added to assembly reactions at $t=0$. The recruitment of specific membrane components was followed by direct immunofluorescence with anti-gp210 and anti-POM121 (Harel et al., 2003b). NPCs were stained with directly labeled mAb414 (Covance), and chromatin with Hoechst 33258 (Sigma-Aldrich). TRITC–NLS–BSA and M9–GFP were added to reconstitution reactions after 1 hour of assembly and samples were removed for analysis after an additional incubation of 15 or 20 minutes. For the separation of nuclear and cytosolic fractions, 25 µl reactions were diluted with 75 µl ELBS, overlaid on 300 µl cushions of 30% sucrose in ELBS and centrifuged in a horizontal rotor at 4000 ***g*** at 4℃ for 8 minutes. Complete recovery of nuclei or nuclear intermediates was verified by Hoechst 33258 staining and the separation of unbound membrane vesicles was determined in equivalent reactions containing labeled membranes. Normalized samples were immunoblotted with specific markers. Poreless, membrane-enclosed intermediates were formed by the addition of 5 mM 1,2-bis(*o*-aminophenoxy)ethane-N,N,N′,N′-tetraacetic acid (BAPTA; Calbiochem) to the reconstitution mixture at $t=0$.

Rescue from BAPTA inhibition was achieved by gentle dilution of the inhibited reaction into two volumes of cytosol, supplemented with recombinant proteins in ELBS and further incubation for 1 hour. To monitor membrane expansion in the interphase mode, nuclei were assembled for 1 hour and samples were removed for staining with Hoechst 33258 and mAb414. At this point the remaining assembly mixture was split into three equal volumes and recombinant proteins were mixed into these reactions. Incubation was continued and samples removed for staining at the 2 and 3 hour time points. Both GST and a zz-histidine-tagged control protein were tested at high concentrations and found to have no effect on nuclear growth rate compared with normal assembly reactions. Nuclei were stained and recorded under identical conditions and the surface area of the NE of 30 randomly chosen nuclei in each category was quantified. The cross-sectional area of each nucleus was measured and multiplied by four to estimate the total NE surface area. See Levi and Heald for validation of the accuracy of this method of measurement (Levi and Heald, 2010). Samples from all assays were fixed in 3% formaldehyde (Electron Microscopy Sciences) in ELB and analyzed by epifluorescence microscopy.

Anchored chromatin assays and epifluorescence microscopy

Anchored chromatin templates for immunofluorescence and immunoblotting were prepared essentially as previously described (Rotem et al., 2009). Briefly, chromatin was decondensed by nucleoplasmin and allowed to settle onto poly-lysine-coated coverslips, washed in ELB (10 mM Hepes pH 7.6, 50 mM KCl, 2.5 mM $MgCl_2$) and blocked in 5% BSA-ELB for 20 minutes. Membrane-free cytosol supplemented with an ATP-regeneration system, 5 µg/ml nocodazole and recombinant proteins, was added to the chromatin-coated coverslips and incubated for 25 minutes at room temperature in a humidified chamber. The coverslips were washed three times with ELBK (10 mM Hepes, pH 7.6, 100 mM KCl, 2.5 mM $MgCl_2$) and then fixed and processed for indirect immunofluorescence, or scraped with SDS-PAGE sample loading buffer for immunoblot analysis. Coverslips were mounted in Fluoromount-G (SouthernBiotech) and recorded on an Olympus BX61TRF motorized microscope, equipped with a UPlanSApo 100× NA 1.4 oil immersion objective and a DP70 digital camera. Images were acquired using the DP Controller and Manager software (Olympus) and figures were prepared in Adobe Photoshop. Quantitative analysis of anti-GST immunofluorescence was performed with OpenView software, as previously described (Rotem et al., 2009; Tsuriel et al., 2006). Hoechst 33258 staining was used to create masks of chromatin surface area, defining relevant pixels in antibody-labeled images. Normalized fluorescence intensity was calculated after the subtraction of non-specific staining and compiled from two independent experiments. Twenty-five randomly chosen, non-overlapping chromatin templates were analyzed in each category.

Field emission scanning electron microscopy (FESEM)

Anchored chromatin templates on silicon chips (Ted Pella, Redding, CA, USA) were prepared as previously described (Rotem et al., 2009) and incubated with reconstitution mixtures, containing cytosol and membranes, for 45 minutes in a humidified chamber. For immunogold labeling, anchored chromatin binding reactions in membrane-free cytosol were probed with anti-GST followed by 12 nm gold-conjugated goat anti-rabbit (Rotem et al., 2009). For the visualization of NPC density after membrane expansion arrest, assembly was carried out in solution, reactions were diluted in 1 ml ELBS and spun down onto silicon chips for 10 minutes at 1000 ***g***. Morphometric analysis of NPC density was performed by counting NPCs in 6–10 approximately flat NE areas of 1×1 µm in two separate experiments. Samples were fixed and further processed for FESEM by critical-point drying on a CPD030 apparatus (Bal-Tec) and sputter coating with 2 nm of chromium (EMITECH K575X) (Rotem et al., 2009). Samples were then viewed on a Zeiss ULTRA *plus* field emission scanning electron microscope, using an in-lens detector for secondary electrons to provide the surface structure and an energy selective backscattered (EsB) detector for backscattered electrons to localize gold particles.

Acknowledgements

The authors thank Douglass Forbes, Ulrike Kutay, Wolfram Antonin and Michael Elbaum for the kind gift of reagents. We also thank Anca Savulescu for critical reading of the manuscript.

Funding

This work was supported by grants from the Israel Science Foundation [grant numbers 813/05 and 1072/10 to A.H.]; and the FESEM work was supported by a training and research grant from the Russell Berrie Nanotechnology Institute – Technion [grant number 2012225 to A.H. and L.S.].

Supplementary material available online at
http://jcs.biologists.org/lookup/suppl/doi:10.1242/jcs.086660/-/DC1

References

Alber, F., Dokudovskaya, S., Veenhoff, L. M., Zhang, W., Kipper, J., Devos, D., Suprapto, A., Karni-Schmidt, O., Williams, R., Chait, B. T. et al. (2007). The molecular architecture of the nuclear pore complex. *Nature* **450**, 695-701.

Anderson, D. J. and Hetzer, M. W. (2008). Shaping the endoplasmic reticulum into the nuclear envelope. *J. Cell Sci.* **121**, 137-142.

Anderson, D. J., Vargas, J. D., Hsiao, J. P. and Hetzer, M. W. (2009). Recruitment of functionally distinct membrane proteins to chromatin mediates nuclear envelope formation in vivo. *J. Cell Biol.* **186**, 183-191.

Antonin, W., Franz, C., Haselmann, U., Antony, C. and Mattaj, I. W. (2005). The integral membrane nucleoporin pom121 functionally links nuclear pore complex assembly and nuclear envelope formation. *Mol. Cell* **17**, 83-92.

Burke, B. and Ellenberg, J. (2002). Remodelling the walls of the nucleus. *Nat. Rev. Mol. Cell Biol.* **3**, 487-497.

Chadrin, A., Hess, B., San Roman, M., Gatti, X., Lombard, B., Loew, D., Barral, Y., Palancade, B. and Doye, V. (2010). Pom33, a novel transmembrane nucleoporin required for proper nuclear pore complex distribution. *J. Cell Biol.* **189**, 795-811.

Chial, H. J., Rout, M. P., Giddings, T. H. and Winey, M. (1998). Saccharomyces cerevisiae Ndc1p is a shared component of nuclear pore complexes and spindle pole bodies. *J. Cell Biol.* **143**, 1789-1800.

Cohen, M., Feinstein, N., Wilson, K. L. and Gruenbaum, Y. (2003). Nuclear pore protein gp210 is essential for viability in HeLa cells and Caenorhabditis elegans. *Mol. Biol. Cell* **14**, 4230-4237.

Cronshaw, J. M., Krutchinsky, A. N., Zhang, W., Chait, B. T. and Matunis, M. J. (2002). Proteomic analysis of the mammalian nuclear pore complex. *J. Cell Biol.* **158**, 915-927.

D'Angelo, M. A., Anderson, D. J., Richard, E. and Hetzer, M. W. (2006). Nuclear pores form de novo from both sides of the nuclear envelope. *Science* **312**, 440-443.

Dawson, T. R., Lazarus, M. D., Hetzer, M. W. and Wente, S. R. (2009). ER membrane-bending proteins are necessary for de novo nuclear pore formation. *J. Cell Biol.* **184**, 659-675.

Doucet, C. M., Talamas, J. A. and Hetzer, M. W. (2010). Cell cycle-dependent differences in nuclear pore complex assembly in metazoa. *Cell* **141**, 1030-1041.

Doye, V. and Hurt, E. (1997). From nucleoporins to nuclear pore complexes. *Curr. Opin Cell Biol.* **9**, 401-411.

Drummond, S. P. and Wilson, K. L. (2002). Interference with the cytoplasmic tail of gp210 disrupts ''close apposition'' of nuclear membranes and blocks nuclear pore dilation. *J. Cell Biol.* **158**, 53-62.

Drummond, S., Ferrigno, P., Lyon, C., Murphy, J., Goldberg, M., Allen, T., Smythe, C. and Hutchison, C. J. (1999). Temporal differences in the appearance of NEP-B78 and an LBR-like protein during Xenopus nuclear envelope reassembly reflect the ordered recruitment of functionally discrete vesicle types. *J. Cell Biol.* **144**, 225-240.

Fahrenkrog, B., Koser, J. and Aebi, U. (2004). The nuclear pore complex: a jack of all trades? *Trends Biochem Sci.* **29**, 175-182.

Fernandez-Martinez, J. and Rout, M. P. (2009). Nuclear pore complex biogenesis. *Curr. Opin Cell Biol.* **21**, 603-612.

Fichtman, B., Ramos, C., Rasala, B., Harel, A. and Forbes, D. J. (2010). Inner/outer nuclear membrane fusion in nuclear pore assembly: biochemical demonstration and molecular analysis. *Mol. Biol. Cell* **21**, 4197-4211.

Forbes, D. J., Kirschner, M. W. and Newport, J. W. (1983). Spontaneous formation of nucleus-like structures around bacteriophage DNA microinjected into Xenopus eggs. *Cell* **34**, 13-23.

Franz, C., Walczak, R., Yavuz, S., Santarella, R., Gentzel, M., Askjaer, P., Galy, V., Hetzer, M., Mattaj, I. W. and Antonin, W. (2007). MEL-28/ELYS is required for the recruitment of nucleoporins to chromatin and postmitotic nuclear pore complex assembly. *EMBO Rep.* **8**, 165-172.

Funakoshi, T., Maeshima, K., Yahata, K., Sugano, S., Imamoto, F. and Imamoto, N. (2007). Two distinct human POM121 genes: requirement for the formation of nuclear pore complexes. *FEBS Lett.* **581**, 4910-4916.

Funakoshi, T., Clever, M., Watanabe, A. and Imamoto, N. (2011). Localization of Pom121 to the inner nuclear membrane is required for an early step of interphase nuclear pore complex assembly. *Mol. Biol. Cell* **22**, 1058-1069.

Gerace, L. and Burke, B. (1988). Functional organization of the nuclear envelope. *Annu. Rev. Cell Biol.* **4**, 335-374.

Gerace, L., Ottaviano, Y. and Kondor-Koch, C. (1982). Identification of a major polypeptide of the nuclear pore complex. *J. Cell Biol.* **95**, 826-837.

Gillespie, P. J., Khoudoli, G. A., Stewart, G., Swedlow, J. R. and Blow, J. J. (2007). ELYS/MEL-28 chromatin association coordinates nuclear pore complex assembly and replication licensing. *Curr. Biol.* **17**, 1657-1662.

Gorsch, L. C., Dockendorff, T. C. and Cole, C. N. (1995). A conditional allele of the novel repeat-containing yeast nucleoporin RAT7/NUP159 causes both rapid cessation of mRNA export and reversible clustering of nuclear pore complexes. *J. Cell Biol.* **129**, 939-955.

Guttinger, S., Laurell, E. and Kutay, U. (2009). Orchestrating nuclear envelope disassembly and reassembly during mitosis. *Nat. Rev. Mol. Cell Biol.* **10**, 178-191.

Hachet, V., Kocher, T., Wilm, M. and Mattaj, I. W. (2004). Importin alpha associates with membranes and participates in nuclear envelope assembly in vitro. *EMBO J.* **23**, 1526-1535.

Hallberg, E., Wozniak, R. W. and Blobel, G. (1993). An integral membrane protein of the pore membrane domain of the nuclear envelope contains a nucleoporin-like region. *J. Cell Biol.* **122**, 513-521.

Harel, A., Chan, R. C., Lachish-Zalait, A., Zimmerman, E., Elbaum, M. and Forbes, D. J. (2003a). Importin beta negatively regulates nuclear membrane fusion and nuclear pore complex assembly. *Mol. Biol. Cell* **14**, 4387-4396.

Harel, A., Orjalo, A. V., Vincent, T., Lachish-Zalait, A., Vasu, S., Shah, S., Zimmerman, E., Elbaum, M. and Forbes, D. J. (2003b). Removal of a single pore subcomplex results in vertebrate nuclei devoid of nuclear pores. *Mol. Cell* **11,** 853-864.

Heath, C. V., Copeland, C. S., Amberg, D. C., Del Priore, V., Snyder, M. and Cole, C. N. (1995). Nuclear pore complex clustering and nuclear accumulation of poly(A)+ RNA associated with mutation of the Saccharomyces cerevisiae RAT2/NUP120 gene. *J. Cell Biol.* **131**, 1677-1697.

Hetzer, M. W. and Wente, S. R. (2009). Border control at the nucleus: biogenesis and organization of the nuclear membrane and pore complexes. *Dev. Cell* **17**, 606-616.

Hetzer, M., Bilbao-Cortes, D., Walther, T. C., Gruss, O. J. and Mattaj, I. W. (2000). GTP hydrolysis by Ran is required for nuclear envelope assembly. *Mol. Cell* **5**, 1013-1024.

Lachish-Zalait, A., Lau, C. K., Fichtman, B., Zimmerman, E., Harel, A., Gaylord, M. R., Forbes, D. J. and Elbaum, M. (2009). Transportin mediates nuclear entry of DNA in vertebrate systems. *Traffic* **10,** 1414-1428.

Lau, C. K., Giddings, T. H., Jr and Winey, M. (2004). A novel allele of Saccharomyces cerevisiae NDC1 reveals a potential role for the spindle pole body component Ndc1p in nuclear pore assembly. *Eukaryot. Cell*. **3**, 447-458.

Lau, C. K., Delmar, V. A., Chan, R. C., Phung, Q., Bernis, C., Fichtman, B., Rasala, B. A. and Forbes, D. J. (2009). Transportin regulates major mitotic assembly events: from spindle to nuclear pore assembly. *Mol. Biol. Cell* **20**, 4043-4058.

Levy, D. L. and Heald, R. (2010). Nuclear size is regulated by importin alpha and Ntf2 in Xenopus. *Cell* **143**, 288-298.

Lohka, M. J. and Masui, Y. (1983). Formation in vitro of sperm pronuclei and mitotic chromosomes induced by amphibian ooplasmic components. *Science* **220**, 719-721.

Macaulay, C. and Forbes, D. J. (1996). Assembly of the nuclear pore: biochemically distinct steps revealed with NEM, GTP gamma S, and BAPTA. *J. Cell Biol.* **132**, 5-20.

Mansfeld, J., Guttinger, S., Hawryluk-Gara, L. A., Pante, N., Mall, M., Galy, V., Haselmann, U., Muhlhausser, P., Wozniak, R. W., Mattaj, I. W. et al. (2006). The conserved transmembrane nucleoporin NDC1 is required for nuclear pore complex assembly in vertebrate cells. *Mol. Cell* **22**, 93-103.

Maul, G. G., Maul, H. M., Scogna, J. E., Lieberman, M. W., Stein, G. S., Hsu, B. Y. and Borun, T. W. (1972). Time sequence of nuclear pore formation in phytohemagglutinin-stimulated lymphocytes and in HeLa cells during the cell cycle. *J. Cell Biol.* **55**, 433-447.

Mitchell, J. M., Mansfeld, J., Capitanio, J., Kutay, U. and Wozniak, R. W. (2010). Pom121 links two essential subcomplexes of the nuclear pore complex core to the membrane. *J. Cell Biol.* **191**, 505-521.

Pemberton, L. F., Rout, M. P. and Blobel, G. (1995). Disruption of the nucleoporin gene NUP133 results in clustering of nuclear pore complexes. *Proc. Natl. Acad. Sci. USA* **92**, 1187-1191.

Rafikova, E. R., Melikov, K., Ramos, C., Dye, L. and Chernomordik, L. V. (2009). Transmembrane protein-free membranes fuse into xenopus nuclear envelope and promote assembly of functional pores. *J. Biol. Chem.* **284**, 29847-29859.

Rasala, B. A., Orjalo, A. V., Shen, Z., Briggs, S. and Forbes, D. J. (2006). ELYS is a dual nucleoporin/kinetochore protein required for nuclear pore assembly and proper cell division. *Proc. Natl. Acad. Sci. USA* **103**, 17801-17806.

Rasala, B. A., Ramos, C., Harel, A. and Forbes, D. J. (2008). Capture of AT-rich chromatin by ELYS recruits POM121 and NDC1 to initiate nuclear pore assembly. *Mol. Biol. Cell* **19**, 3982-3996.

Rotem, A., Gruber, R., Shorer, H., Shaulov, L., Klein, E. and Harel, A. (2009). Importin beta regulates the seeding of chromatin with initiation sites for nuclear pore assembly. *Mol. Biol. Cell* **20**, 4031-4042.

Ryan, K. J., Zhou, Y. and Wente, S. R. (2007). The karyopherin Kap95 regulates nuclear pore complex assembly into intact nuclear envelopes in vivo. *Mol. Biol. Cell* **18**, 886-898.

Sasagawa, S., Yamamoto, A., Ichimura, T., Omata, S. and Horigome, T. (1999). In vitro nuclear assembly with affinity-purified nuclear envelope precursor vesicle fractions, PV1 and PV2. *Eur. J. Cell Biol.* **78**, 593-600.

Schwartz, T. U. (2005). Modularity within the architecture of the nuclear pore complex. *Curr. Opin Struct. Biol.* **15**, 221-226.

Siniossoglou, S., Wimmer, C., Rieger, M., Doye, V., Tekotte, H., Weise, C., Emig, S., Segref, A. and Hurt, E. C. (1996). A novel complex of nucleoporins, which includes Sec13p and a Sec13p homolog, is essential for normal nuclear pores. *Cell* **84**, 265-275.

Stavru, F., Hulsmann, B. B., Spang, A., Hartmann, E., Cordes, V. C. and Gorlich, D. (2006a). NDC1: a crucial membrane-integral nucleoporin of metazoan nuclear pore complexes. *J. Cell Biol.* **173**, 509-519.

Stavru, F., Nautrup-Pedersen, G., Cordes, V. C. and Gorlich, D. (2006b). Nuclear pore complex assembly and maintenance in POM121- and gp210-deficient cells. *J. Cell Biol.* **173**, 477-483.

Tsuriel, S., Geva, R., Zamorano, P., Dresbach, T., Boeckers, T., Gundelfinger, E. D., Garner, C. C. and Ziv, N. E. (2006). Local sharing as a predominant determinant of synaptic matrix molecular dynamics. *PLoS Biol.* **4**, e271.

Ulbert, S., Platani, M., Boue, S. and Mattaj, I. W. (2006). Direct membrane protein-DNA interactions required early in nuclear envelope assembly. *J. Cell Biol.* **173**, 469-476.

Vasu, S. K. and Forbes, D. J. (2001). Nuclear pores and nuclear assembly. *Curr. Opin Cell Biol.* **13**, 363-375.

Vasu, S., Shah, S., Orjalo, A., Park, M., Fischer, W. H. and Forbes, D. J. (2001). Novel vertebrate nucleoporins Nup133 and Nup160 play a role in mRNA export. *J. Cell Biol.* **155**, 339-354.

Vigers, G. P. and Lohka, M. J. (1991). A distinct vesicle population targets membranes and pore complexes to the nuclear envelope in Xenopus eggs. *J. Cell Biol.* **112**, 545-556.

Vollmar, F., Hacker, C., Zahedi, R. P., Sickmann, A., Ewald, A., Scheer, U. and Dabauvalle, M. C. (2009). Assembly of nuclear pore complexes mediated by major vault protein. *J. Cell Sci.* **122**, 780-786.

Walther, T. C., Askjaer, P., Gentzel, M., Habermann, A., Griffiths, G., Wilm, M., Mattaj, I. W. and Hetzer, M. (2003). RanGTP mediates nuclear pore complex assembly. *Nature* **424**, 689-694.

Weis, K. (2003). Regulating access to the genome: nucleocytoplasmic transport throughout the cell cycle. *Cell* **112**, 441-451.

Wente, S. R. and Blobel, G. (1994). NUP145 encodes a novel yeast glycine-leucine-phenylalanine-glycine (GLFG) nucleoporin required for nuclear envelope structure. *J. Cell Biol.* **125**, 955-969.

Wozniak, R. and Clarke, P. R. (2003). Nuclear pores: sowing the seeds of assembly on the chromatin landscape. *Curr. Biol.* **13**, R970-R972.

Wozniak, R. W., Bartnik, E. and Blobel, G. (1989). Primary structure analysis of an integral membrane glycoprotein of the nuclear pore. *J. Cell Biol.* **108**, 2083-2092.

Yavuz, S., Santarella-Mellwig, R., Koch, B., Jaedicke, A., Mattaj, I. W. and Antonin, W. (2010). NLS-mediated NPC functions of the nucleoporin Pom121. *FEBS Lett.* **584**, 3292-3298.